Fabrication and Characteristics of High-Speed Oxide-Confined VCSELs Using InGaAsP–InGaP Strain-Compensated MQWs

Ya-Hsien Chang, H. C. Kuo, *Member, IEEE*, Fang-I. Lai, Yi-An Chang, C. Y. Lu, L. H. Laih, and S. C. Wang, *Senior Member, IEEE*

***Abstract*—This paper presents the fabrication and characteristics of high-performance 850-nm InGaAsP–InGaP strain-compensated multiple-quantum-well (MQW) vertical-cavity surface-emitting lasers (VCSELs). The InGaAsP–InGaP MQW's composition was optimized through theoretical calculations, and the growth condition was optimized using photoluminescence. These VCSELs exhibit superior performance with characteristics threshold currents ∼0.4 mA and slope efficiencies ∼0.6 mW/mA. The threshold current change with temperature is less than 0.2 mA, and the slope efficiency drops less than ∼30% when the substrate temperature is raised from room temperature to 85 °C. A high modulation bandwidth of 14.5 GHz and a modulation current efficiency factor of 11.6 GHz/(mA)$^{1/2}$ are demonstrated. The authors have accumulated life test data up to 1000 h at 70 °C/8 mA.**

***Index Terms*—High-speed electronics, InGaAsP–InGaP, strain-compensated, vertical-cavity surface-emitting lasers (VCSELs).**

I. Introduction

Currently 850-nm oxide-confined vertical-cavity surface-emitting lasers (VCSELs) have become a standard technology for application in local area networks (LANs) from 1.25 to 10 Gb/s [1]–[4]. The low-threshold current, high modulation bandwidth, and high modulation current efficiency make VCSELs an ideal source for high-speed optical communication [5]–[7]. The low divergent angle and circular beam lead to efficiency fiber coupling and simpler packaging. The surface emission from the VCSELs also facilitates the two-dimensional array integration and allows wafer level testing, which in turn leads to low fabrication cost. The use of an Al-free InGaAsP-based active region is an attractive alternative to the conventional (Al)GaAs active region for infrared (IR) VCSELs. While edge-emitting diode lasers with Al-free active regions have demonstrated performance and reliability surpassing AlGaAs-active devices [8], [9]. In addition, theoretical calculations have predicted a lower transparency current density, high differential gain, and better temperature performance in InGaAsP-strain active VCSELs in respect to lattice-matched GaAs quantum-well active devices [10]. These parameters are all very important in high-speed and high-temperature VCSEL design because the relaxation resonance frequency of the laser depends on the square root of the differential gain as well as the difference of operation current and threshold current [4]. The use of tensile-strained barriers like $In_{0.4}Ga_{0.6}P$ can provide strain compensation and reduce active region carrier leakage. Al-free materials are significantly less reactive to the oxide level, compared to AlGaAs materials, which make them ideal for the reliable manufacture process [8]. Proton-implanted VCSELs using strain $In_{0.18}Ga_{0.82}As_{0.8}P_{0.2}$ active region has demonstrated good performance [11]. Recently, we demonstrated high-speed modulation up to 12.5 Gb/s from 25 °C to 85 °C utilizing $In_{0.18}Ga_{0.82}As_{0.8}P_{0.2}$–$In_{0.4}Ga_{0.6}P$strain-compensated multiple-quantum-well (SC-MQWs) VCSELs [12].

This paper reports on the fabrication and characteristics of high-performance 850-nm InGaAsP–InGaP SC-MQW VCSELs. Small-signal, dc, and large-signal measurements were performed on SC-MQWs VCSELs. Finally, the initial reliability data from these VCSELs are presented.

II. Theory

Comparing the InGaAsP–InGaP SC-MQWs and GaAs–AlGaAs quantum wells (QWs), the gain spectrum and material gain as a function of carrier density were calculated based on the $k \cdot p$ theory with a valence banding mixing effect. An 8×8 Lutttinger–Kohn Hamiltonian matrix is used in this investigation. The method is followed by Chuang [13], and the gain spectral is broadened by Lorentzian's function. The well width and MQW's compositions were both set as 8 nm and $In_{0.18}Ga_{0.82}As_{0.8}P_{0.2}$–$In_{0.4}Ga_{0.6}P$ to tune the emission wavelength to 842 nm. A scheme of the conduction band diagram was shown in Fig. 1. The obtained gain spectrum and material gain were compared with a conventional GaAs–$Al_{0.26}Ga_{0.74}As$ MQWs using the same algorithm. The conduction band offsets of $In_{0.18}Ga_{0.82}As_{0.8}P_{0.2}$–$In_{0.4}Ga_{0.6}P$ and GaAs–$Al_{0.26}Ga_{0.74}As$ are assumed to be 0.5 and 0.65, respectively. The calculation of bandgap energy formula is adapted from a Varshni equation with $\alpha = 5.5 \times 10^{-4}$ eV/K, $\beta = 225$ K for both InGaAsP and AlGaAs materials, and the bandgap is adapted to the value at 298 K. Although the Varshni parameters might not be the same for InGaAsP and AlGaAs, the

Manuscript received April 15, 2004; revised July 12, 2004. This work was supported in part by the National Science Council, Republic of China, under Contract NSC-90-2215-E009-088, the Academic Excellence Program of the Ministry of Education of the Republic of China under Contract 88-FA06-AB, and the Institute of Nuclear Energy Research under Contract 922001InER015.

Y.-H. Chang, H. C. Kuo, F.-I. Lai, Y.-A. Chang, C. Y. Lu, and S. C. Wang are with the Institute of Electro-Optical Engineering, National Chiao-Tung University, Hsin-chu, Taiwan, R.O.C. (e-mail: hckuo@faculty.nctu.edu.tw).

L. H. Laih is with M-Comm Corporation, Hsin-chu, Taiwan, R.O.C.

Digital Object Identifier 10.1109/JLT.2004.834835

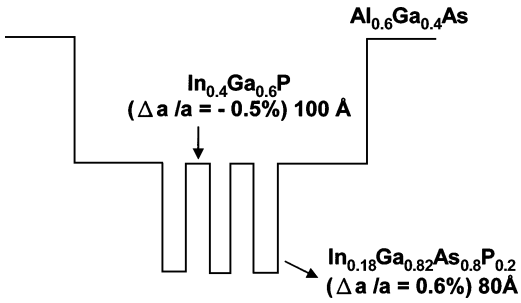

Fig. 1. Schematic energy bandgap diagram for $In_{0.18}Ga_{0.82}As_{0.8}P_{0.2}$–$In_{0.4}Ga_{0.6}P$—active region.

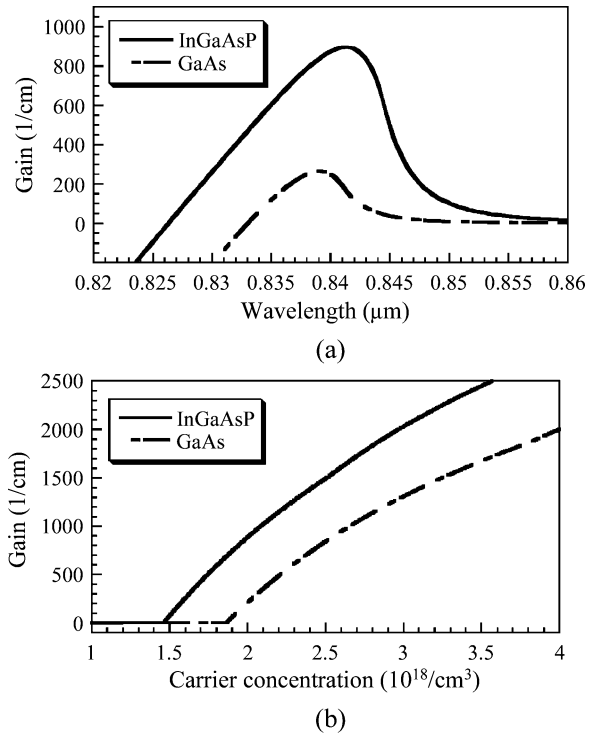

Fig. 2. Material gain spectrum and material gain as a function of carrier density of $In_{0.18}Ga_{0.82}As_{0.8}P_{0.2}$–$In_{0.4}Ga_{0.6}P$ MQW and $GaAs$–$Al_{0.26}Ga_{0.74}As$ MQW.

error incurred is likely tolerable because the small bandgap deviation should not affect the material gain. As shown in Fig. 2(a), the material gain of $In_{0.18}Ga_{0.82}As_{0.8}P_{0.2}$–$In_{0.4}Ga_{0.6}P$ is approximately triple that of the $GaAs$–$Al_{0.26}Ga_{0.74}As$ structure when the input carrier concentration is 2×10^{18} cm^{-3}. The material gains of $In_{0.18}Ga_{0.82}As_{0.8}P_{0.2}$–$In_{0.4}Ga_{0.6}P$ and $GaAs$–$Al_{0.26}Ga_{0.74}As$ as a function of the input carrier concentration are depicted in Fig. 2(b). The transparent carrier concentrations of $In_{0.18}Ga_{0.82}As_{0.8}P_{0.2}$–$In_{0.4}Ga_{0.6}P$ and $GaAs$–$Al_{0.26}Ga_{0.74}As$ are 1.5×10^{18} cm^{-3} and 1.78×10^{18} cm^{-3}, respectively. Furthermore, $In_{0.18}Ga_{0.82}As_{0.8}P_{0.2}$–$In_{0.4}Ga_{0.6}P$ provides higher gain than $GaAs$–$Al_{0.26}Ga_{0.74}As$ in the entire calculation range. The results obtained numerically suggest that the high-material-gain low-transparency carrier concentration make the InGaAsP SC-MQWs a better active layer. In addition, its superior performance has been confirmed in edge-emitting lasers [8], [9].

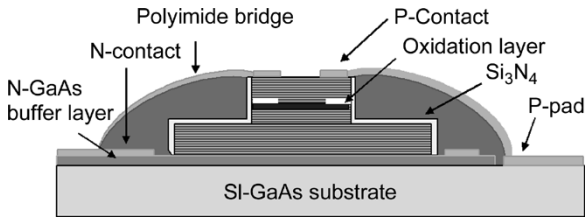

Fig. 3. Schematic cross section of high-speed VCSEL structure.

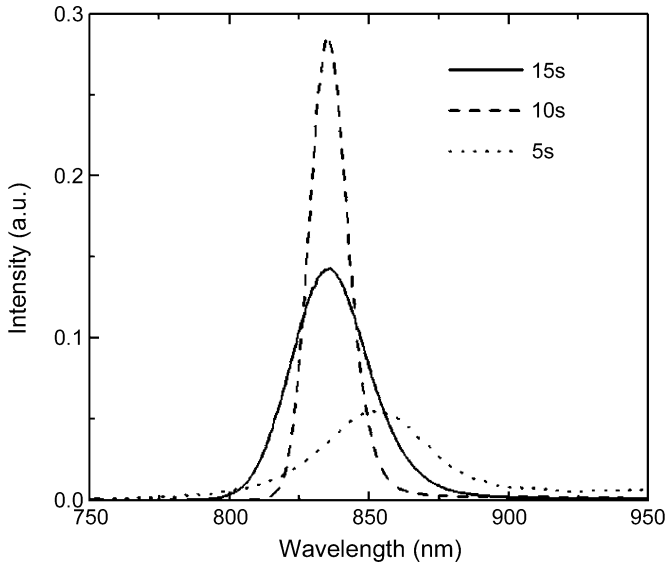

Fig. 4. PL spectra of SC-MQW with different growth interruption times.

III. Experiment

The schematic structure of a fabricated top emitting VCSEL is shown in Fig. 3, which has been grown by low-pressure metal organic chemical vapor deposition (MOCVD) on a semi-insulating (100) GaAs substrate. The group-V precursors are the hydride sources AsH_3 and PH_3. The trimethyl alkyls of gallium (Ga), aluminum (Al), and indium (In) are the group-III precursors. The dopant sources are Si_2H_6 and CBr_4 for the n and p dopants. The bottom n-type distributed Bragg reflector (DBR) consists of 35-period $Al_{0.15}Ga_{0.85}As$–$Al_{0.9}Ga_{0.1}As$. The top p-type DBR consists of 23 pairs of $Al_{0.15}Ga_{0.85}As$–$Al_{0.9}Ga_{0.1}As$. The active layer consists of three $In_{0.18}Ga_{0.82}As_{0.8}P_{0.2}$–$In_{0.4}Ga_{0.6}P$ (80 Å/100 Å) SC-MQWs surrounded by a $Al_{0.6}Ga_{0.4}As$ cladding layer to 1λ cavity. A 30-nm-thick $Al_{0.98}Ga_{0.02}As$ was introduced on the upper cavity spacer layer to form an oxide confinement. Finally, 1λ thickness of the current spreading layer and heavily doped GaAs ($p > 2 \times 10^{19}$ cm^{-3}) contacting layer was grown. The n-type DBR was grown at 750 °C. The QW region and p-type DBR were grown at 650 °C. Growth interruptions of 5, 10, or 15 s were introduced before and after $In_{0.18}Ga_{0.82}As_{0.8}P_{0.2}$ QW growth. Fig. 4 shows the comparison of photoluminescence spectra of $In_{0.18}Ga_{0.82}As_{0.8}P_{0.2}$–$In_{0.4}Ga_{0.6}P$ with different growth interruption times. The 5-s growth interruption is not enough to evacuate residual As in the growth reactor, resulting in the carryover of As into the $In_{0.4}Ga_{0.6}P$ barrier. The 15-s growth interruption is so long that some impurities can be gettered at

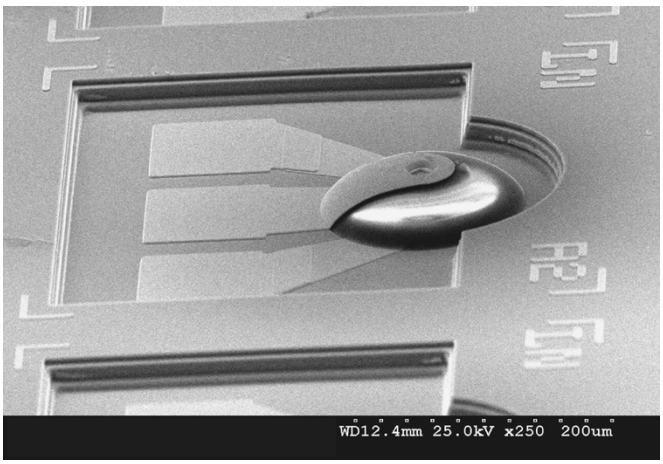

Fig. 5. SEM picture of the finished VCSEL.

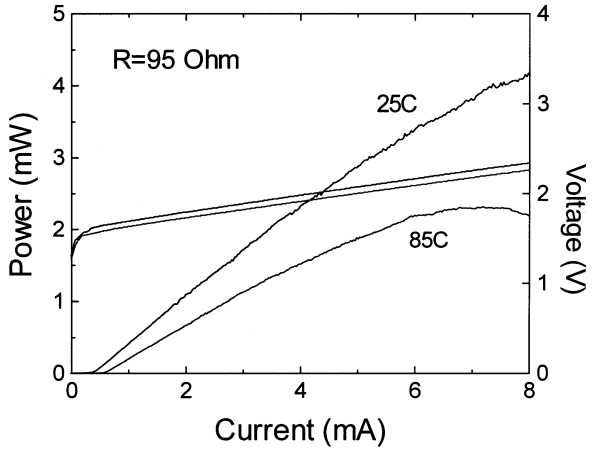

Fig. 6. SC-MQW InGaAsP–InGaP VCSEL light output and LIV curves at room temperature and 85 °C.

the interface or indium segregation after strained layer growth, resulting in the degradation of luminescence. The 10-s growth interruption seems to give the best luminescence quality. The composition of SC-MQWs is characterized by a high-resolution X-ray diffraction. The gain peak position $=$ 835 nm was determined by photoluminescence while the FP-dip wavelength $=$ 842 nm was determined by reflection measurement. The VCSELs were fabricated utilizing the processing described by Peters *et al.* to minimize capacitance while keeping reasonably low resistance [3]. The processing sequence included six photomasks to fabricate polyimide-planarized VCSELs with coplanar waveguide probe pads. Device fabrication began with the formation of cylindrical mesas of 20 μm in diameter by etching the surrounding semiconductor to the bottom n-type mirror to a depth of 5 μm using a reactive ion etching (RIE) system. The sample was wet-oxidized in a 420 °C steam environment for $\sim$12 min to form the current aperture and provide lateral index guiding to the lasing mode. The oxidation rate was 0.6 μm/min for the $Al_{0.98}Ga_{0.02}As$ layer, so the oxide-extended 7.5 μm from the mesa sidewall. The VCSELs therefore have a 5-μm-diameter emitting aperture defined by lateral oxidation. A 40-μm circular mesa was formed after oxidation using wet chemical etching $(H_2O : H_2SO_4 : H_2O_2 = 8:1:8)$ down to the n-buffer layer. Following Si_3N_4 was deposited for passivation. Ti/Au was evaporated for the p-type contact ring, and AuGeNi/Au was evaporated onto the etched n-buffer layer to form the n-type contact, which is connected to the semi-insulating substrate. Contacts were alloyed for 30 s at 420 °C using RTA. After contact formation, photosensitive polyimide was spun on the sample for field insulation and planarization. Ti/Au with thicknesses of 200/3000 Å were deposited for metal interconnects and coplanar waveguide probe-bond pads. Heat treatment after the metal deposition was utilized to improve metal-to-polyimide adhesion strength. Fig. 5 shows the scanning electron microscope (SEM) photo of a finished VCSEL.

IV. Results and Discussion

Fig. 6 shows the typical light output and voltage versus current (LIV) curves of the SC-MQW InGaAsP–InGaP VCSEL at room temperature and 85 °C under continuous-wave operation. These VCSELs exhibit kink-free current-light output performance with threshold currents $\sim$0.4 mA and slope efficiencies $\sim$0.6 mW/mA. The threshold current change with temperature is less than 0.2 mA, and the slope efficiency drops by less than $\sim$30% when the substrate temperature is raised from room temperature to 85 °C. This is superior to the properties of GaAs–AlGaAs VCSELs with similar size [14]. The resistance of our VCSELs is $\sim$95 Ω, and capacitance is $\sim$0.1 pF. As a result, the devices are limited by the parasitics to a frequency response of approximately 15 GHz. The lateral mode characteristics is an important feature since it strongly affects the transmission properties. Fig. 7 shows the emission spectrum of a VCSEL at an operating current of 6 mA. This spectrum was recorded with an optical spectrum analyzer (Advantest 8381 A) with a spectral resolution of 0.1 nm. Two dominate modes were observed at 844.2 and 843.7 nm. The root-mean-square (rms) spectral linewidths at 2, 6, and 8 mA are 0.15, 0.37, and 0.4 nm, respectively, which can fulfill the requirement $(<= 0.45$ nm$)$ of 10-Gb/s data transmission [15].

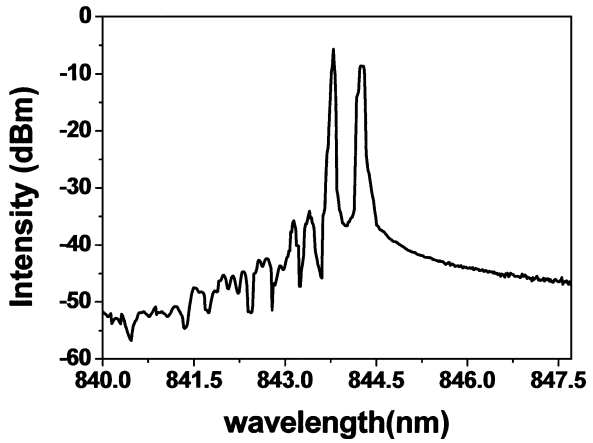

Fig. 7. Optical spectrum at 6 mA of the VCSEL.

The small-signal response of VCSELs as a function of bias current was measured using a calibrated vector network analyzer (Agilent 8720ES) with on-wafer probing and 50-μm multimode optical fiber connected to a New Focus 25-GHz photodetector. Fig. 8 shows the measured (dashed lines) and fitted

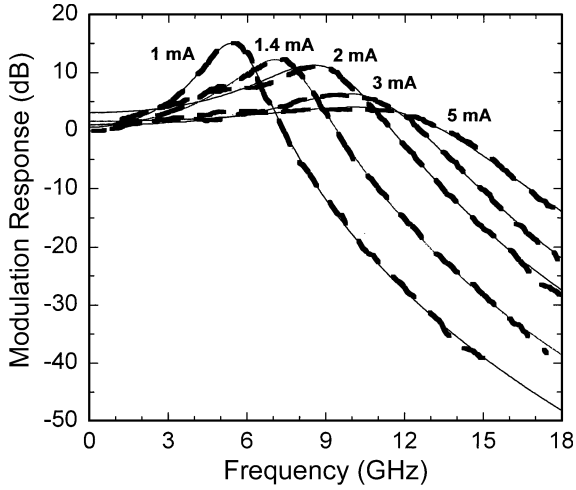

Fig. 8. Small-signal modulation responses of a 5-μm-diameter VCSEL at different bias current levels.

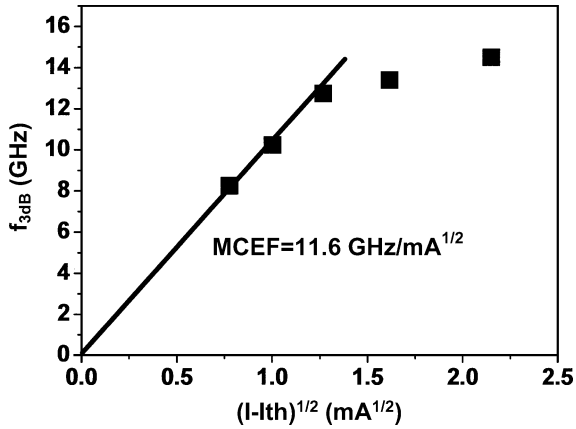

Fig. 9. 3-dB frequency as a function of square root of current above threshold current.

(solid lines) small-signal frequency response of a 5-μm VCSEL at different bias current levels. The modulation frequency is increased with increasing bias current until flattening at a bias of approximately 5 mA. With only 3 mA (5 mA) of bias current, the maximum 3-dB modulation frequency response is measured to be ~13 (14.5) GHz at 25 °C and is suitable for 12.5-Gb/s operation. The measured data were fit to a general three-pole modulation transfer function [16], [17]

$$H(f) = C\left(\frac{fr^2}{fr^2 - f^2 + j\frac{f}{2\pi}\gamma}\right)\left(\frac{1}{1 + j\left(\frac{f}{fp}\right)}\right)$$

where f is the modulation frequency, f_p is the parasitic roll-off frequency, f_r is the resonant frequency, and γ is the damping rate.

Fig. 9 shows the 3-dB modulation frequency as a function the square root of the difference in the current above threshold. The relaxation resonance frequency is found saturate for driving currents above 3 mA. By fitting the lowest current points in Fig. 8, we obtain a modulation current efficiency of 11.6 GHz/$(\text{mA})^{1/2}$ [18]. This is higher than GaAs–AlGaAs VCSELs with similar size [6], [19] and is comparable with

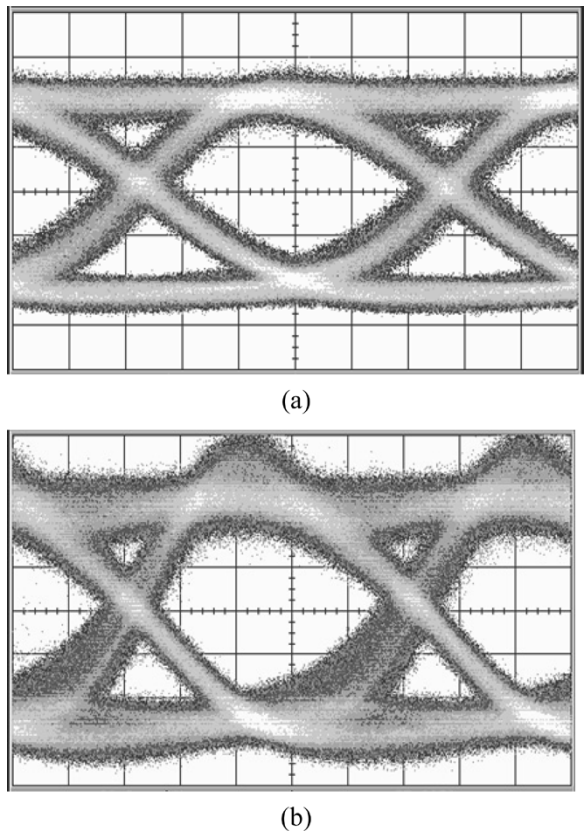

Fig. 10. (a) 25 °C and (b) 85 °C eye diagram of SC-VCSEL up to 12.5 Gb/s with 6-dB extinction ratio. The scale in the figure is 15 ps/div.

oxide-confined VCSELs with InGaAs-based QWs [7], [16]. Plotting the damping rate γ versus f_r^2 reveals a K-factor of 0.3 ns. Neglecting heating effects and external parasitics, the intrinsic bandwidth was found to be 29.6 GHz using the relation $f_{\max} = \sqrt{2}(2\pi/K)$.

To measure the high-speed VCSEL under large-signal modulation, microwave and lightwave probes were used in conjunction with a 12.5-Gb/s pattern generator and a 12-GHz photoreceiver. The eye diagrams were taken for back-to-back transmission on SC-MQW InGaAsP–InGaP VCSELs. As shown in Fig. 10(a), the room temperature eye diagram of our VCSEL biased at 4 mA with data up to 12.5 Gb/s and a 6-dB extinction ratio has a clear open eye pattern indicating good performance of the VCSELs. The rise time T_r is 28 ps, and the fall time T_f is 41 ps with jitter $(p - p) = 20$ ps. The VCSELs also show superior performance at high temperature. Fig. 10(b) demonstrated the high-speed performance of our VCSELs (biased at 5 mA) with reasonably open eye diagrams at 12.5 Gb/s and a 6-dB extinction ratio at 85 °C. This further confirms the superior performance of our VCSELs.

Guaranteeing device reliability is always difficult but a natural task for the components supplier in the data communication markets. We have accumulated life test data up to 1000 h at 70 °C/8 mA with exceptional reliability. As shown in Fig. 11, the light output is plotted versus time scale for SC-MQW VCSEL chips under the high-temperature operation lifetime (HTOL) test at 70 °C/8 mA. None of them shows abnormal behavior.

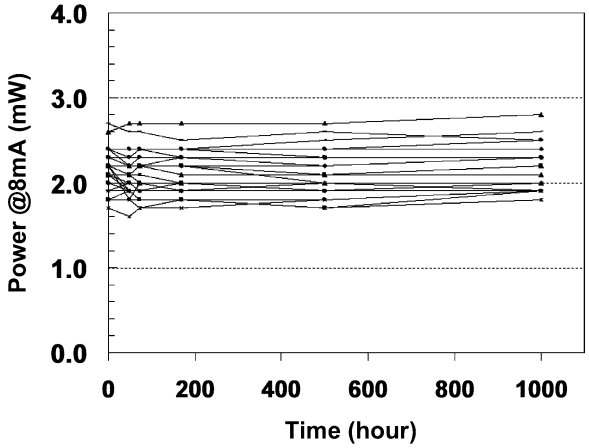

Fig. 11. HTOL (70 °C/8 mA) performance of the strain-compensated VCSEL.

V. Conclusion

The superior performance of InGaAsP–GaAsP MQW was demonstrated numerically and experimentally. High-performance SC-MQW VCSELs were realized with low threshold current, good temperature performance, and high-frequency response and good reliability. All of these advantages make the SC-MQW VCSELs promising for OC-192 commercial applications

Acknowledgment

The authors would like to thank Dr. C. P. Kuo of LuxNet Corporation, Dr. I. H. Tan of AXT, Prof. Nelson Tansu of Lehigh University, and Dr. C. P. Sung from ITRI for useful discussions and technical support.

References

[1] J. A. Tatum, A. Clark, J. K. Guenter, R. A. Hawthorne, and R. H. Johnson, "Commercialization of Honeywell's VCSEL technology," in *Proc. Vertical-Cavity Surface-Emitting Lasers IV, SPIE*, K. D. Choquette and C. Lei, Eds., pp. 2–13.

[2] F. H. Peters and M. H. MacDougal, "High-speed high-temperature operation of vertical-cavity surface-emitting lasers," *IEEE Photon. Technol. Lett.*, vol. 13, pp. 645–647, July 2001.

[3] F. H. Peters, D. J. Welch, V. Jayaraman, M. H. MacDougal, J. D. Tagle, T. A. Goodwin, J. E. Schramm, T. D. Lowes, S. P. Kilcoyne, K. R. Nary, J. S. Bergey, and W. Carpenter, "10 Gb/s VCSEL-based data links," Photonics West, San Jose, CA, Tech. Rep. OE 3946-26, 2000.

[4] C. W. Wilmsen, H. Temkin, and L. A. Coldren, Eds., *Vertical-Cavity Surface-Emitting Lasers: Design, Fabrication, Characterization, and Applications*. Cambridge, U.K.: Cambridge Univ. Press, 1999.

[5] K. L. Lear, M. Ochiai, V. M. Hietala, H. Q. Hou, B. E. Hammons, J. J. Banas, and J. A. Nevers, "High-speed vertical cavity surface emitting lasers," in *Dig. IEEE/LEOS Summer Topical Meetings*, Aug. 1997, pp. 53–54.

[6] J. A. Lehman, R. A. Morgan, M. K. Hibbs-Brenner, and D. Carlson, "High-frequency modulation characteristics of hybrid dielectric/AlGaAs mirror singlemode VCSELs," *Electron. Lett.*, vol. 31, pp. 1251–1252, 1995.

[7] K. L. Lear, A. Mar, K. D. Choquette, S. P. Kilcoyne, R. P. Schneider Jr., and K. M. Geib, "High-frequency modulation of oxide confined vertical cavity surface emitting lasers," *Electron. Lett.*, vol. 32, pp. 457–458, 1996.

[8] L. J. Mawst, S. Rusli, A. Al-Muhanna, and J. K. Wade, "Short-wavelength ($0.7\ \mu\text{m} < \lambda < 0.78\ \mu\text{m}$) high-power InGaAsP-active diode lasers," *IEEE J. Select. Topics Quantum Electron.*, vol. 5, pp. 785–791, May–June 1999.

[9] N. Tansu, D. Zhou, and L. J. Mawst, "Low temperature sensitive, compressively-strained InGaAsP active ($\lambda = 0.78$–$0.85\ \mu\text{m}$) region diode lasers," *IEEE Photon. Technol. Lett.*, vol. 12, pp. 603–605, June 2000.

[10] T. E. Sale, C. Amamo, Y. Ohiso, and T. Kurokawa, "Using strained lasers (AlGa) InAsP system materials to improve the performance of 850 nm surface- and edge-emitting lasers," *Appl. Phys. Lett.*, vol. 71, pp. 1002–1004, 1997.

[11] N. Tansu and L. J. Mawst, "Compressively-strained InGaAsP-active ($\lambda = 0.85\ \mu\text{m}$) VCSELs," in *IEEE Lasers Electro-Optics Society 2000 Annu. Meeting (LEOS 2000)*, vol. 2, Nov. 2000, pp. 724–725.

[12] H. C. Kuo, Y. S. Chang, F. I. Lai, and T. H. Hsueh, "High speed modulation of 850 nm InGaAsP/InGaP strain-compensated VCSELs," *Electron. Lett.*, vol. 39, pp. 1051–10 523, 2003.

[13] S. L. Chuang, "Efficient band-structure calculation of strained quantum-wells," *Phys. Rev. B*, vol. 43, pp. 9649–9661, 1991.

[14] *Proc. Production High-Speed Oxide Confined VCSEL Arrays for Datacom Application, SPIE*, vol. 4649, 2002, p. 142.

[15] . [Online]. Available: http://www.ieee802.org/

[16] B. J. Thibeault, K. Bertilsson, and E. R. Hegblom, "High-speed characteristics of low-optical loss oxide-aperture vertical-cavity laser," *IEEE Photon. Technol. Lett.*, vol. 9, pp. 11–13, Jan. 1997.

[17] L. A. Coldren and S. W. Corzine, *Diode Lasers and Photonic Integrated Ciurcuits*. New York: Wiley, 1995, pp. 201–204.

[18] T. R. Chen, B. Zhao, L. Eng, and Y. H. Zhuang, "Very high modulation efficiency of ultralow threshold current single quantum well InGaAs lasers," *Electron. Lett.*, vol. 29, pp. 1525–1526, 1993.

[19] S. Eitel, S. Hunziker, and D. Vez, "Multimode VCSEL's for high bitrate and transparent low-cost fiber-optic links," in *Proc. SPIE*, vol. 4649, 2002, p. 183.

Ya-Hsien Chang was born in Taipei, Taiwan, on January 12, 1976. He received the B.S. and M.S. degrees in electrical engineering from National Tsing-Hua University, Hsin-chu, Taiwan, R.O.C. He is currently working toward the Ph.D. degree at the Institute of Electro-Optical Engineering, National Chiao-Tung University, Hsin-chu, Taiwan, R.O.C.

His research focuses on characterizing III-nitride material and modeling the high-speed vertical-cavity surface-emitting lasers (VCSELs).

H. C. Kuo (S'94–M'99) received the B.S. degree in physics from National Taiwan University, Taipei, Taiwan, R.O.C., in 1990, the M.S. degree in electrical and computer engineering from Rutgers University, Piscataway, NJ, in 1995, and the Ph.D. degree in electrical and computer engineering from University of Illinois–Urbana Champaign in 1999.

He has an extensive professional career both in research and industrial research institutions, which includes being a Research Consultant with Lucent Technologies, Bell Laboratories (1995–1997), a Research and Development Engineer with the Fiber-Optics Division at Agilent Technologies (1999–2001), and Research and Development Manager with LuxNet Corporation (2001–2002). Since September 2002, he joined National Chiao-Tung University, Hsin-chu, Taiwan, , R.O.C., as a Faculty Member of the Institute of Electro-Optical Engineering. He has authored or coauthored more than 60 publications. His current research interests include the epitaxy, design, fabrication, and measurement of high-speed InP- and GaAs-based vertical-cavity surface-emitting lasers, as well as GaN-based light-emitting devices and nanostructures.

Fang-I. Lai was born in Kaohsiung City, Taiwan, R.O.C., on October 4, 1975. She received the B.S. degree in physics from Tung-Hai University, Taiwan, R.O.C., and the M.S. degree from the Institute of Electro-Optical Engineering, National Chiao-Tung University, Taiwan, R.O.C. She is currently working toward the Ph.D. degree at the same university.

Her research focuses on the study of process techniques of III–V vertical-cavity surface-emitting lasers.

Yi-An Chang was born in Taipei, Taiwan, on March 13, 1978. He received the B.S. and M.S. degrees in physics from National Changhua University of Education (NCUE), Changhua, Taiwan, R.O.C., in 2001 and 2003, respectively. Since 2003, he has been working toward the Ph.D. degree at the Institute of Electro-Optical Engineering, National Chiao-Tung University, Hsin-chu, Taiwan, R.O.C.

He joined the Laboratory of Lasers and Optical Semiconductors at NCUE in 2000, where he was engaged in research on passive Q switching with solid-state saturable absorbers and III-nitride semiconductor materials for light-emitting diodes and semiconductor lasers under the instruction of Prof. Y.-K. Kuo. His recent research interests include III-nitride and InGaAsN semiconductor lasers.

C. Y. Lu received the B.S. degree in electrical engineering from Yuan Ze University, Chungli, Taiwan, , R.O.C.. He is currently working toward the M.S. degree at the Semiconductor Laser Technology Laboratory, Institute of Electro-Optical Engineering, National Chiao-Tung University, Hsin-chu, Taiwan, R.O.C.

His research focuses on characterizing and modeling high-speed vertical-cavity surface-emitting lasers.

L. H. Laih, photograph and biography not available at the time of publication.

S. C. Wang (M'79–SM'03) received the B.S. degree from National Taiwan University, Taipei, Taiwan, R.O.C., the M.S. degree from National Tohoku University, Sendai, Japan, and the Ph.D. degree from Stanford University, Stanford, CA, in 1971, all in electrical engineering.

He has an extensive professional career both in academic and industrial research institutions, which includes being a Faculty Member at the National Chiao-Tung University, Hsin-chu, Taiwan, R.O.C. (1965–1967); a Research Associate at Stanford University (1971–1974); a Senior Research Scientist at Xerox Corporation (1974–1985); and a Consulting Scientist at Lockheed-Martin Palo Alto Research Laboratories (1985–1995). In 1995, he rejoined National Chiao-Tung University as a Faculty Member of the Institute of Electro-Optical Engineering. He has authored or coauthored more than 160 publications. His current research interests include semiconductor lasers, vertical-cavity surface-emitting lasers, blue and ultraviolet lasers, quantum-confined optoelectronic structures, optoelectronic materials, diode-pumped lasers, and semiconductor laser applications.